Design of RF Structures for the Demonstrator

Dario Giove *(INFN-LASA)*
Luigi Celona, Gino Sorbello and Davide Guarnera (INFN-LNS and University of Catania), Elisa Del Core (INFN-LASA)

Funded by the European Union (EU). Views and opinions expressed are however those of the author only and do not necessarily reflect those of the EU or European Research Executive Agency (REA). Neither the EU nor the REA can be held responsible for them.

Summary

- Cooling channel description and principle overview
- Cooling channel main elements
- RF cells and main parameters
- A first prototype of 3 cavity RF cell structure for the demonstrator
- Technological issues and test stand to obtain experimental data

Muon collider and RF system challenges

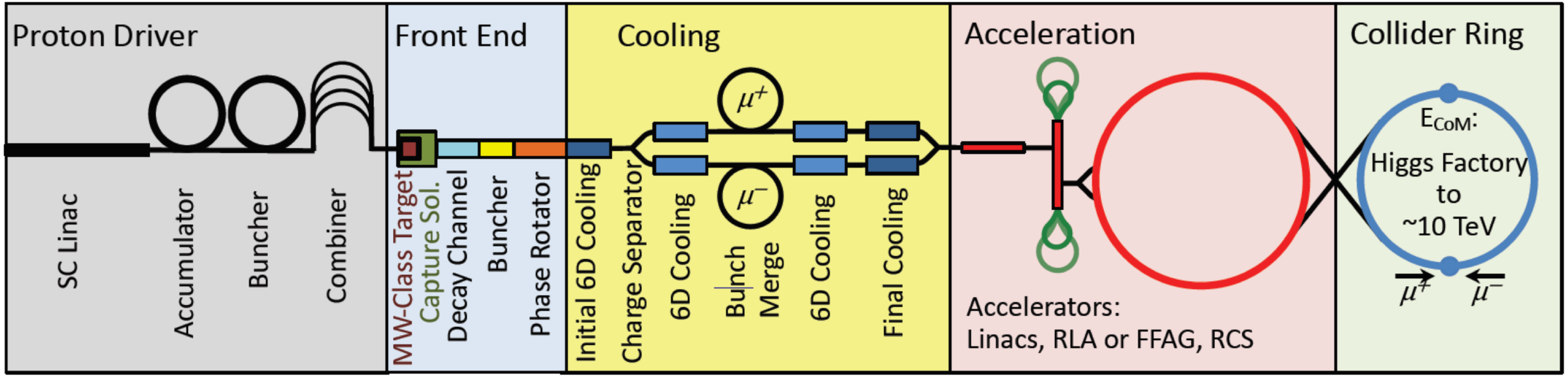

The main challenges of a muon collider design are those arising from the short muon lifetime, which is 2.2 μs at rest, and the difficulty of producing large numbers of muons in bunches with small emittance.

The purpose of the cooling cell is to provide a reduction of the normalized transverse emittance by almost three orders of magnitude (from 1 × 10−2 to 5 × 10−5 m-rad), and a reduction of the longitudinal emittance by one order of magnitude of the Muon Beam generated by the collision of a proton beam with a production target, resulting in a shower of pions that will then decay into muons. Pions are generated with a large angular spread, and a large momentum spread as well.

Cooling cell scheme

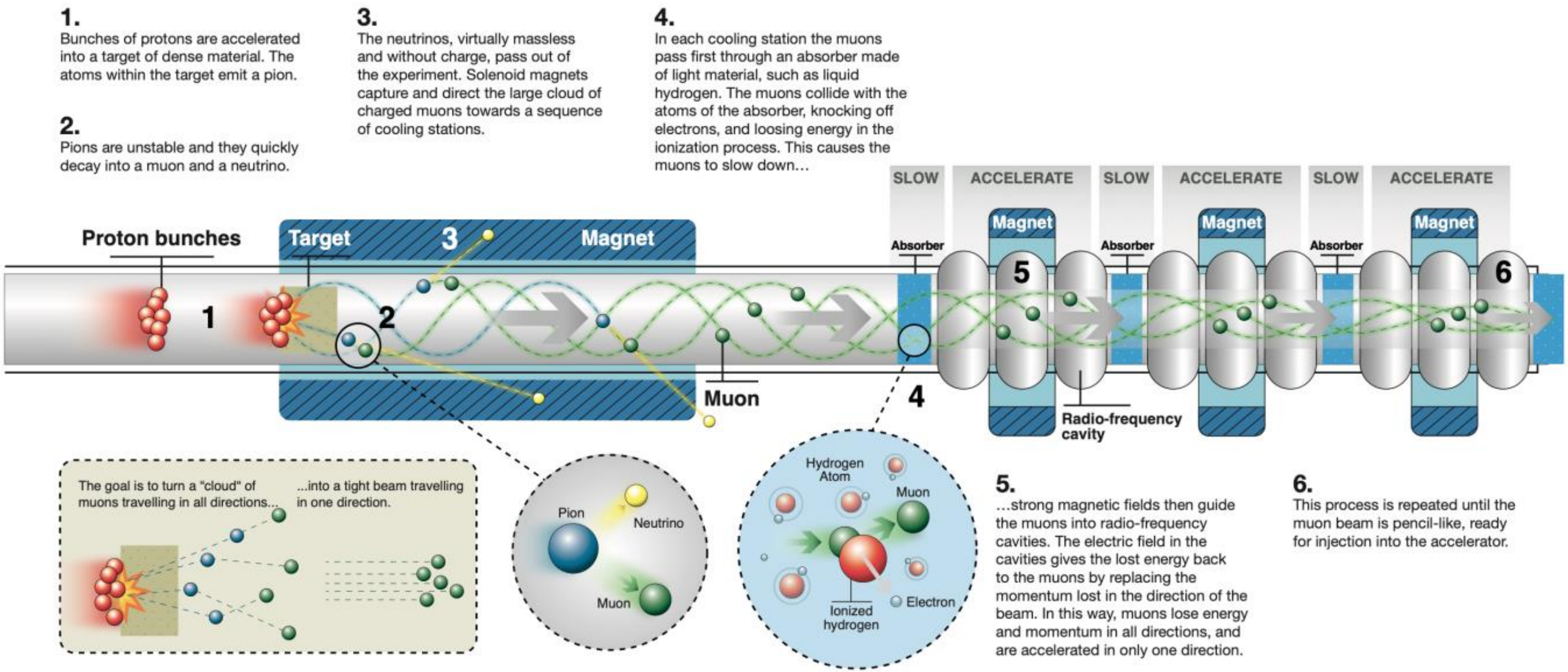

Fig. 3: Principle of the Muon Ionisation Cooling

Terminology

Before to discuss the panorama of the open points related to RF and the activities carried out in the last year, a definition of the terminology that we will use in the discussions has been defined.

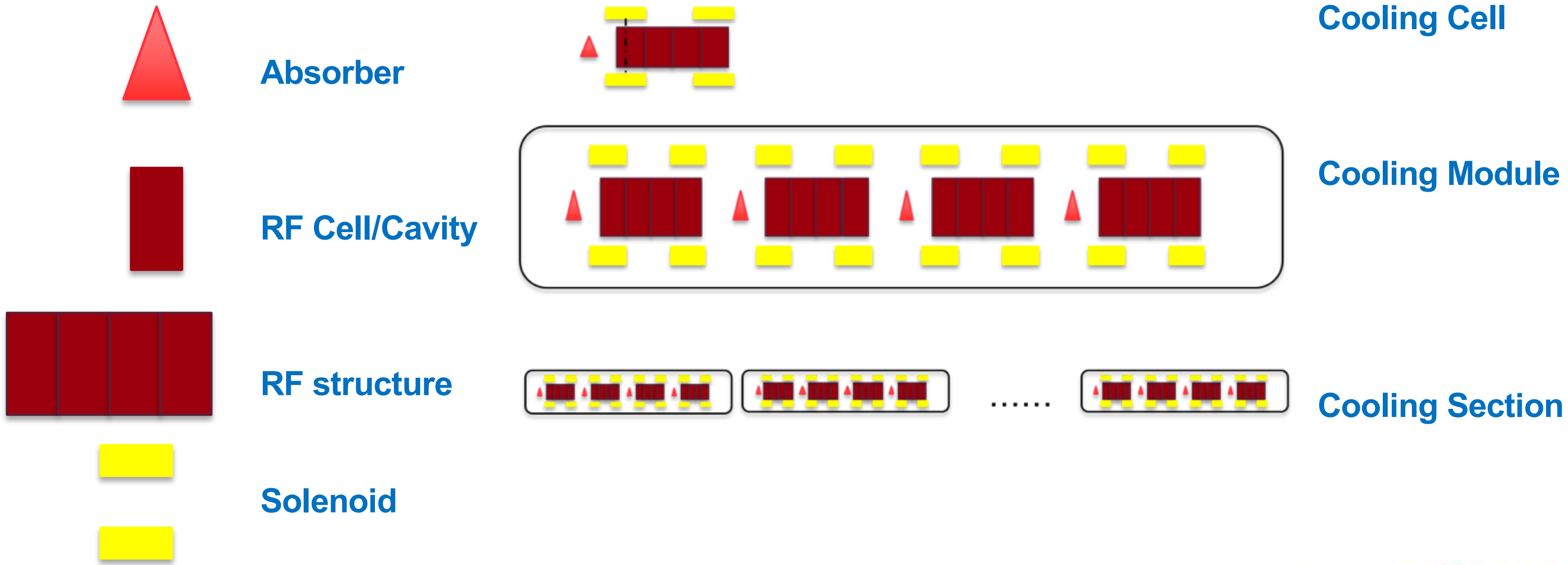

RF Cavity and RF Structure Design

A decision on the type of RF structure that will have to integrated in the cell requires taking into account a number of parameters that may be summarized as in the following:

- **the RF frequency**
- **the required real estate gradient of the electric field in a cell vs. the peak gradient achievable in the RF structure**
- **expected breakdown rate and eventual mitigation strategy, especially in the high magnetic field and high magnetic gradient they experience**
- **specific materials and surface treatments for the cavity bodies.**
- **the type of RF coupling from cell to cell in a RF structure**
- **the space available to fit ancillaries (e.g. tuners, power couplers, cooling pipes etc…), considering the tight interference with the cryomagnetic system**
- **the available or realistically feasible power sources**

Most of the parameters being used for simulations of the entire cooling section are at the edge or beyond the present state-of-the-art, therefore require careful evaluation of the feasibility of the corresponding technological solution.

RF cell @704 MHz INFN studies

5 Cavity Design Parametrization and FoMs

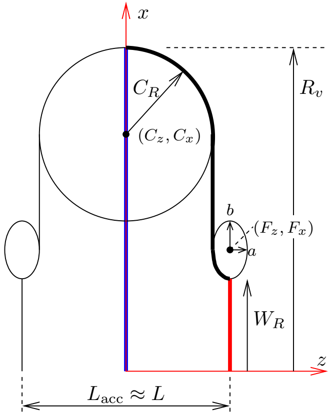

Figure 1: Adopted geometrical parametrization for the cavity designed.

Table 1: Geometrical parameters, $L_{acc} = 187.8$, $f_0 = 704$ MHz (see Fig. 1)

Descript.	param.	value (mm)
Cavity length (external)	L_{acc}	187.8
Cavity radius	R_v	181.85
Aluminum window radius	W_R	60
Aluminum window thickness	W_T	0.3
Ellipse z semi-axis (fillet)	a	5
Ellipse x semi-axis (fillet)	b	11
Derived:		
Cavity length (internal)	$L = L_{acc} - W_T \approx L_{acc}$	
Top circle curvature radius	$C_R = L/2 - a$	$--$
Top circle center x-coord.	$C_x = 0$	$--$
Top circle center y-coord.	$C_y = R - C_R$	$--$

Table 2: FoMs of the designed cavity. $E_{in} = 39.5$ J (Energy stored in the full cavity)

Descrp.	Param.	Unit	INFN
Transit Time	T		0.645
Aver. Nom. gradient	E_0	MV/m	44
Accelerating gradient	E_{acc}	MV/m	28.35
Quality Factor (eig.)	Q_0		39352
Effect. Shunt Impedance	r_{eff}	MΩ	6.39
Effective R over Q	r_{eff}/Q	Ω	162.3
Dissipated power	P_{diss}	MW	4.44

7 New Flat-Top Cavity Design; Geometrical Parametrization and FoMs

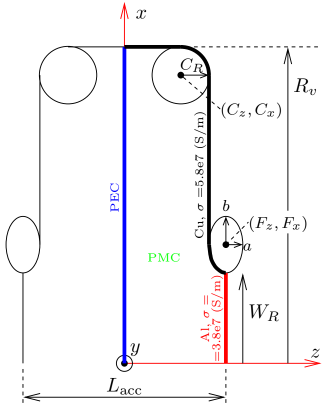

Table 3: Geometrical parameters, $L_{acc} = 187.8$, $f_0 = 704$ MHz (see Fig. 8)

Descript.	param.	value (mm)
Cavity length (external)	L_{acc}	187.8
Cavity radius	R_v	164.9
Aluminium window radius	W_R	60
Aluminium window thickness	W_T	0.3
Ellipse z semi-axis (fillet)	a	5
Ellipse x semi-axis (fillet)	b	11
Top circle curv. radius (fillet)	C_R	12
Derived:		
Cavity length (internal)	$L = L_{acc} - W_T \approx L_{acc}$	
Top circle center z-coord.	$C_z = L/2 - a - C_R$	$--$
Top circle center x-coord.	$C_x = R_v - C_R$	$--$
Ellipse circle center z-coord.	$F_z = L/2 - a$	$--$
Ellipse circle center x-coord.	$F_x = W_R + b$	$--$

Table 4: FoMs of the designed cavity. $E_{in} = 38$ J (Energy stored in the full cavity)

Descrp.	Param.	Unit	INFN
Transit Time	T		0.643
Aver. Nom. gradient	E_0	MV/m	44
Accelerating gradient	E_{acc}	MV/m	28.26
Quality Factor (eig.)	Q_0		35630
Effect. Shunt Impedance	r_{eff}	MΩ	6
Effective R over Q	r_{eff}/Q	Ω	167.6
Dissipated power	P_{diss}	MW	4.71

Table 5: FoMs comparison between the round-top design and the flat-top design

Descrp.	Param.	round-top	flat-top
Stored Energy	E_{in} (J)	37.8	37.5
Transit Time	T	0.644	0.643
Aver. Nom. gradient	E_0 (MV/m)	44	44
Accelerating gradient	E_{acc} (MV/m)	28.35	28.26
Quality Factor (eig.)	Q_0	39352	35630
Eff. Shunt Impedance	r_{eff} (MΩ)	6.38	5
Effective (R over Q)	r_{eff}/Q (Ω)	162.3	167.6
Dissipated power	P_{diss} (MW)	4.44	4.71

Comparison Between Round-Top and Flat-Top cavities

$$P_{in} = 1,15 \text{ MW (ref. stage 5)}$$

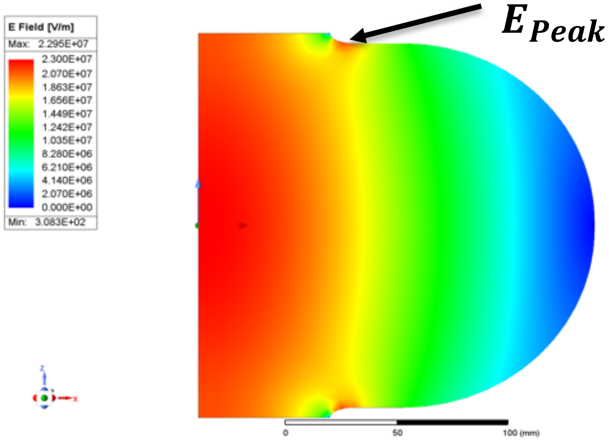

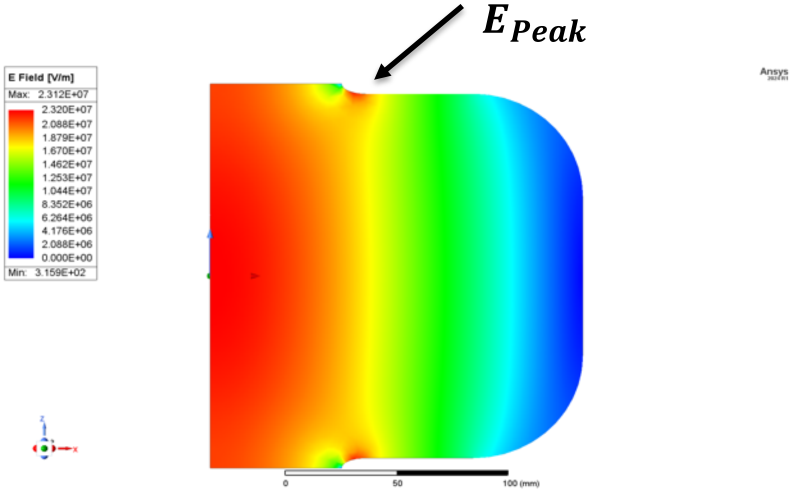

$$\frac{E_{Peak}}{E_{acc}} \approx 1.30; \quad \frac{E_{Peak}}{E_0} \approx 1$$

$$\frac{E_{Peak}}{E_{acc}} \approx 1.60; \quad \frac{E_{Peak}}{E_0} \approx 1,03$$

Flat-Top Cavity Geometry

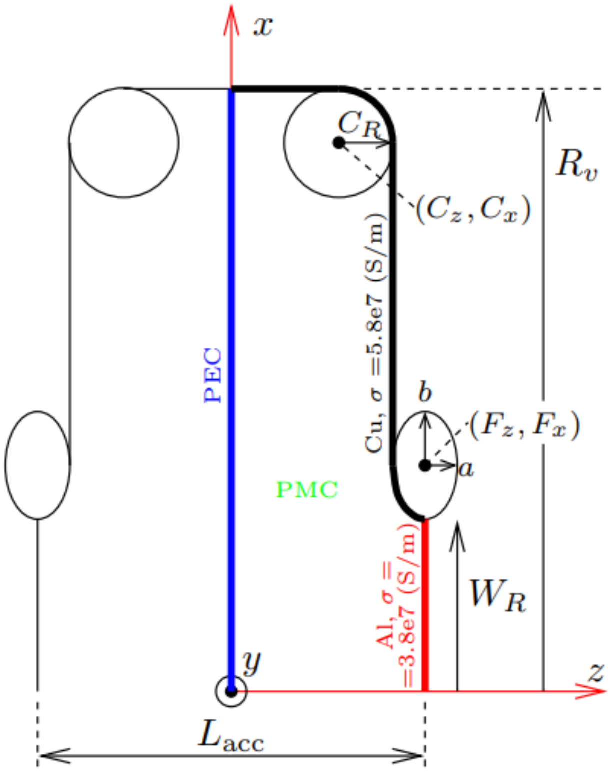

Description	Parameter	Value
Cavity length (external)	L_{acc}	$187.8\ mm$
Cavity radius	R_v	$170.2\ mm$
Aluminium window radius	W_R	$60\ mm$
Aluminium window thickness	W_T	$0.05 - 0.3\ mm$
Ellipse z semi − axis (fillet)	a	$5\ mm$
Ellipse x semi − axis (fillet)	b	$10\ mm$
Top circle curv. radius (fillet)	C_R	$50\ mm$
Cavity length (internal)	$L = L_{acc} - W_T \approx L_{acc}$	
Top circle center z − coord	$C_z = L/2 - a - C_R$	
Top circle center x-coord	$C_x = R_v - C_R$	
Ellipse circle center z-coord	$F_z = L/2 - a$	
Ellipse circle center x-coord	$F_x = W_R + b$	

Comparison Between Electric and Magnetic Coupling

Description	Parameter	Electric Coupling (Periodic, Eigen)	Magnetic Coupling (Eigen)
Stored Energy	E_{in} (J)	22	10
Transit Time	T	0.765	0.643
Aver. Nom. Gradient	E_0 (MV/m)	22, 5	22, 5
Accelerating Gradient	E_{acc} (MV/m)	17.21	14,46
Quality Factor (eigen)	Q_0	38829	38345
Eff. Shunt Impedance	r_{eff} (MΩ)	4,17	6,41
Effective (R over Q)	$\frac{r_{eff}}{Q}$ (Ω)	107,54	167,15
Dissipated Power	P_{diss} (MW)	2,51	1,15

3 cells RF preliminary structure

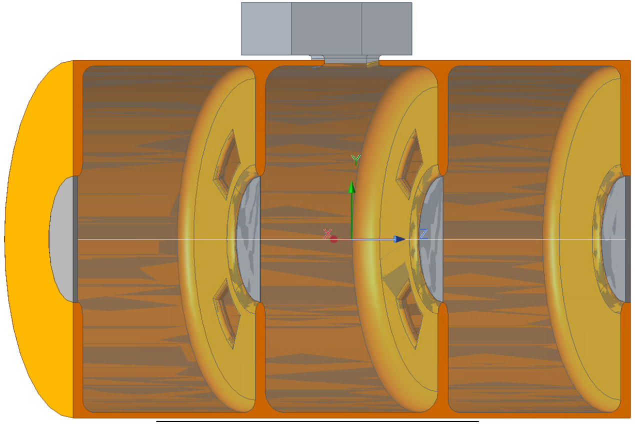

Figure 14: Preliminary design of 3 connected Flat-Top cells fed by waveguide.

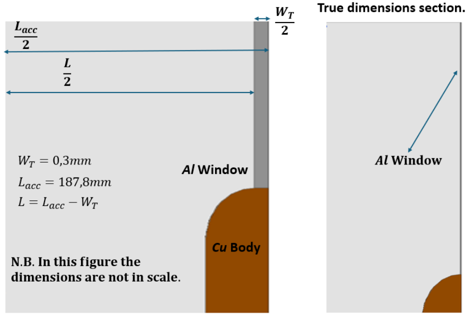

Figure 11: Section of the Aluminum window

WAVEGUIDE WR-1150

- Recommended Frequency Band: 0. 63 to 0. 97 GHz
- Cutoff Frequency of Lowest Order Mode: 0. 513 GHz
- Dimension: [292. 1; 146. 05] mm

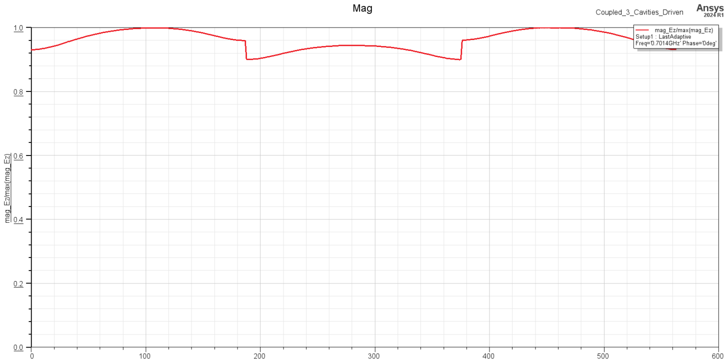

3 cells RF preliminary structure

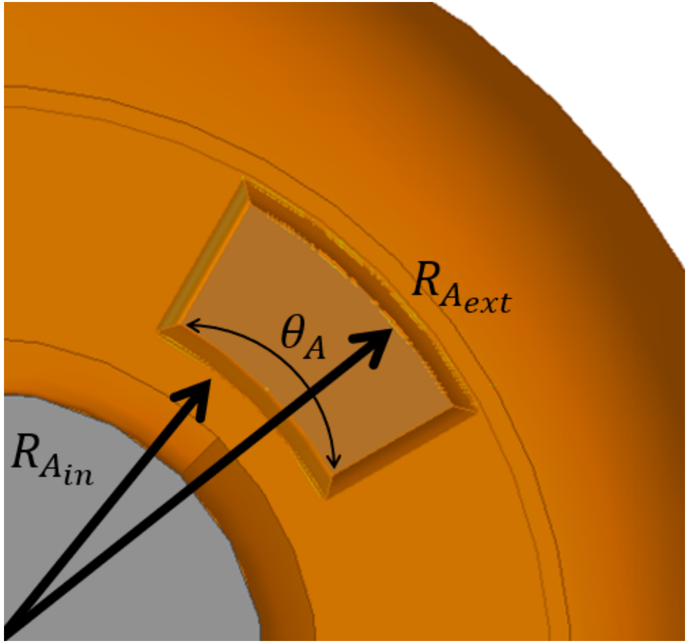

The coupling has been achived by exploiting four slots spaced 90° degrees apart.

Table 6: Geometrical parameters, $L_{acc} = 187.8$, $f_0 = 704$ MHz (see Fig. 8)

Descript.	param.	value	
Cavity length (external)	L_{acc}	187.8	mm
Cavity radius	R_v	170.2	mm
Aluminium window radius	W_R	60	mm
Aluminium window thickness	W_T	0.3	mm
Ellipse z semi-axis (fillet)	a	5	mm
Ellipse x semi-axis (fillet)	b	11	mm
Top circle curv. radius (fillet)	C_R	50	mm
Inner slot Radius	$R_{A_{in}}$	85	mm
External coupling slot Radius	$R_{A_{ext}}$	113.5	mm
Angular coupling slot Span	θ_A	15	deg
Fillet coupling slot		4	mm
Derived:			
Cavity length (internal)	$L = L_{acc} - W_T \approx L_{acc}$		
Top circle center z-coord.	$C_z = L/2 - a - C_R$		$--$
Top circle center x-coord.	$C_x = R_v - C_R$		$--$
Ellipse circle center z-coord.	$F_z = L/2 - a$		$--$
Ellipse circle center x-coord.	$F_x = W_R + b$		$--$

L_{acc} is chosen equal to $L_{ref} = 187.8$ mm for π-mode operation at $f = 704$ MHz. R_v is tuned to have $f = 704$ MHz.

3 cells RF preliminary mechanical design

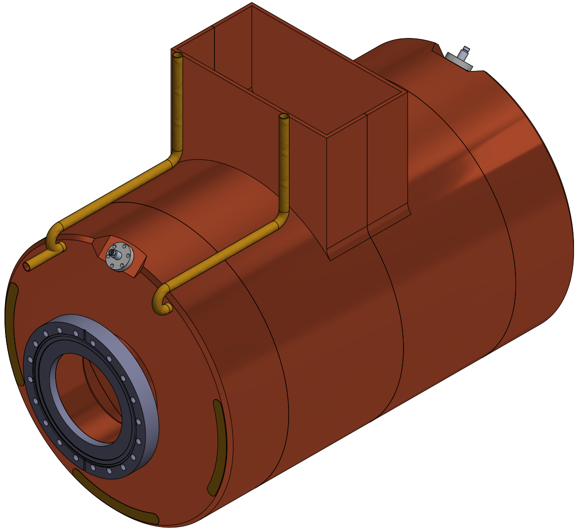

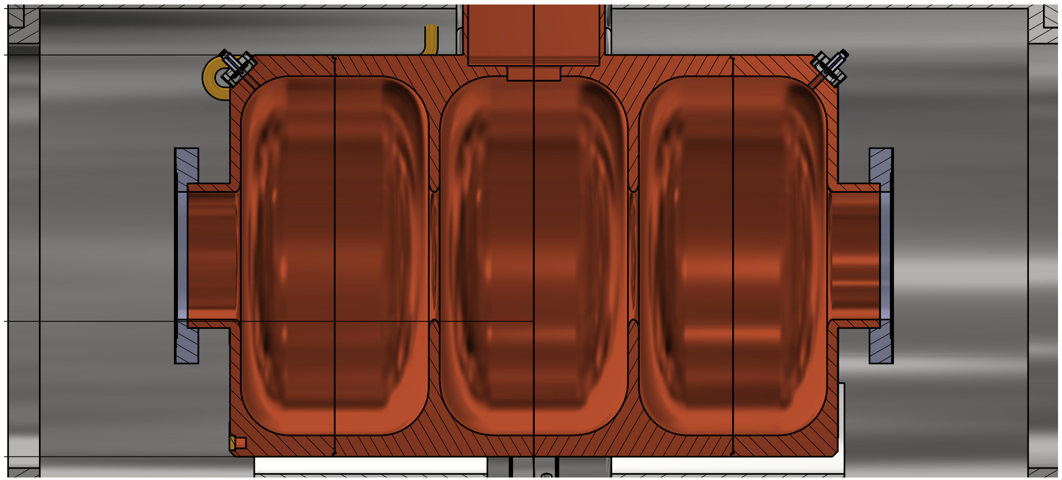

Copper weight: 180 kg
8 water channels
Max. external diameter: less than 500 mm

Expected RF Breakdown Rate and Mitigation Strategy in High Magnetic Fields

High voltage breakdown in both vacuum and gas has been studied extensively. The presence of a multi-tesla external magnetic field provided a new variable, however. As ionization cooling depends on RF cavities operating in such an environment, the performance of said cavities must be understood and characterized.

Early experiments focused on 805 MHz vacuum RF cavities.

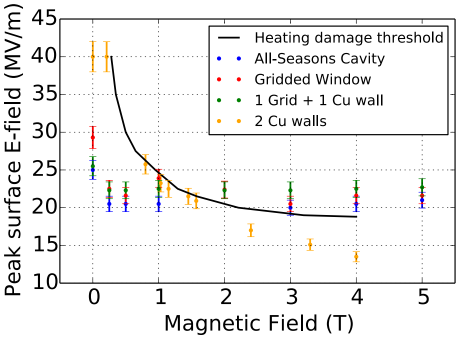

Figure 3: Peak surface electric field vs. external, applied *B*-field for cavity configurations described above. The black line indicates the threshold for surface fracture from beamlet heating, as discussed in [4].

RF BREAKDOWN OF 805 MHZ CAVITIES IN STRONG MAGNETIC FIELDS*

D. Bowring, A. Kochemirovskiy, M. Leonova, A. Moretti, M. Palmer, D. Peterson, K. Yonehara, FNAL, Batavia, IL 60150, USA
B. Freemire, P. Lane, Y. Torun, IIT, Chicago, IL 60616, USA
D. Stratakis, BNL, Upton, NY 11973, USA
A. Haase, SLAC, Menlo Park, CA 94025, USA

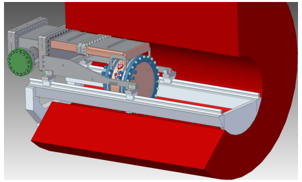

Bowring et al, PRAB 23 072001, 2020

Material	*B*-field (T)	*E*-field (MV/m)
Cu	0	24.4 ± 0.7
Cu	3	12.9 ± 0.4
Be	0	41.1 ± 2.1
Be	3	$> 49.8 \pm 2.5$

Changeable Cu/Be walls

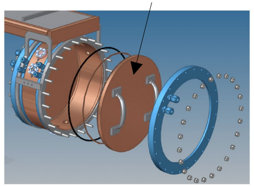

Materials and Treatments

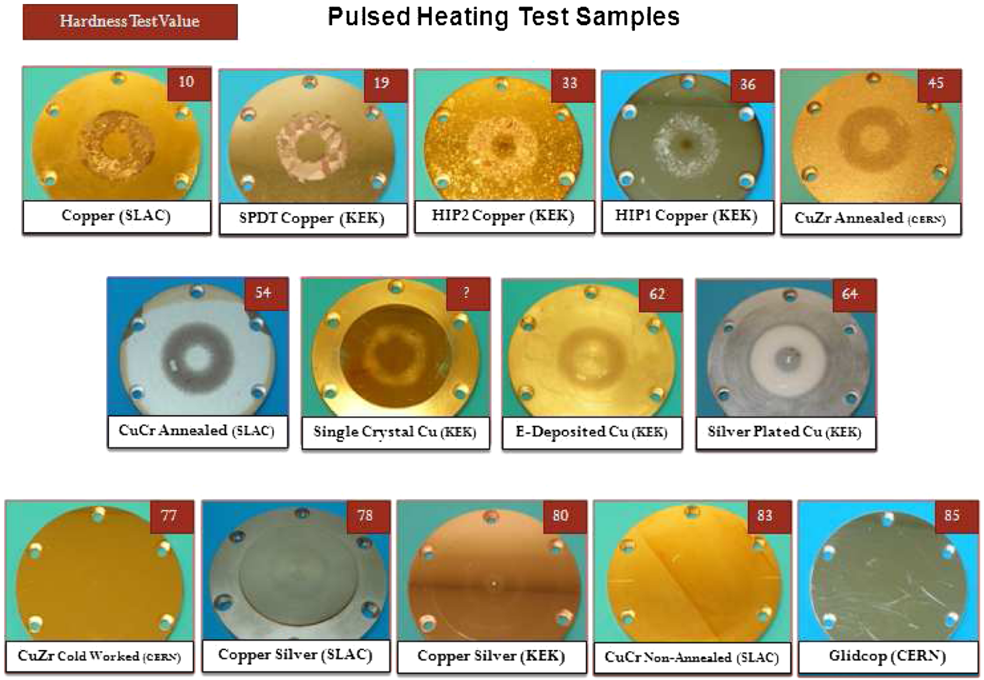

The surface damage due to pulsed heating was significantly more pronounced on the softer materials that are shown on the top row

Technologies for build- ing accelerator structures made from the harder copper alloys are not yet completely developed but some testing in single cell structures has been conducted that shows some improvement over pure copper

Experimental study of rf pulsed heating

Lisa Laurent,* Sami Tantawi, Valery Dolgashev, and Christopher Nantista
SLAC National Accelerator Laboratory, 2575 Sand Hill Road, Menlo Park, California 94025, USA

Yasuo Higashi
KEK, High Energy Accelerator Research Organization, 1-1 Oho, Tsukuba, Ibaraki 305-0801, Japan

Markus Aicheler, Samuli Heikkinen, and Walter Wuensch
CERN, European Organization for Nuclear Research, 1211 Geneva 23, Switzerland

(Received 9 September 2010; published 7 April 2011)

E-field in High Magnetic Gradients

Why we are proposing to carry out tests in a DC based environment ?

- **Simple setup with respect to a RF based one**
- **Tests faster and more flexible**
- **Study on materials and surface treatments**
- **Additional input for further RF based experimental campaigns**
- **Field levels of the order of 100 MV/m (over max. 0.1 mm gp)**
- **Energy similar to the one involved in RF**
- **UHV conditions**
- **BD initial phenomena very similar**

We already have a possible setup (magnet @ 1 T with a 120 mm bore and HV power supplies, radiation detectors, experience on data and image acquisition and competence in material treatments)

1. study of innovative materials to create electrodes to be tested with a high DC static field in the presence of a magnetic field of at least 1 T or higher
2. study of surface finishing, coating and cleaning techniques for the above materials
3. DC high static field test in the presence of a magnetic field of at least 1 T or higher

E-field in High Magnetic Gradients

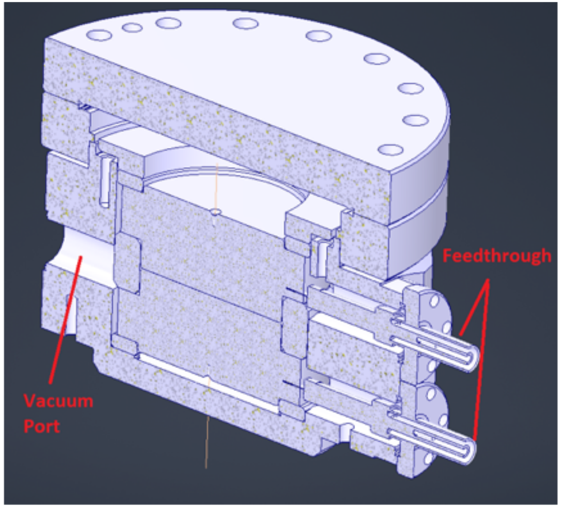

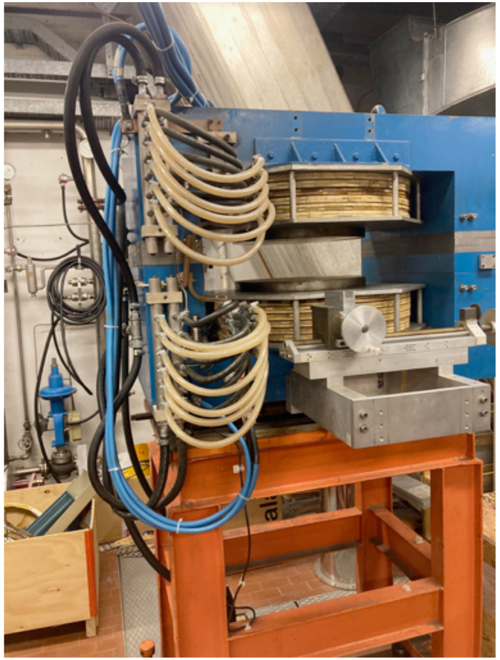

The PVX-4110 pulse generator is a direct coupled, air cooled, solid state half-bridge (totem pole) design, offering equally fast pulse rise and fall times, low power dissipation, and virtually no over-shoot, undershoot or ringing. It has overcurrent detection and shutdown circuitry to protect the pulse generator from potential damage due to arcs and shorts in the load or interconnect cable.

Suitable to test different materials, surface finishing and treatments up to 50 MV/m

A 3 GHz Proposal designed at INFN LASA

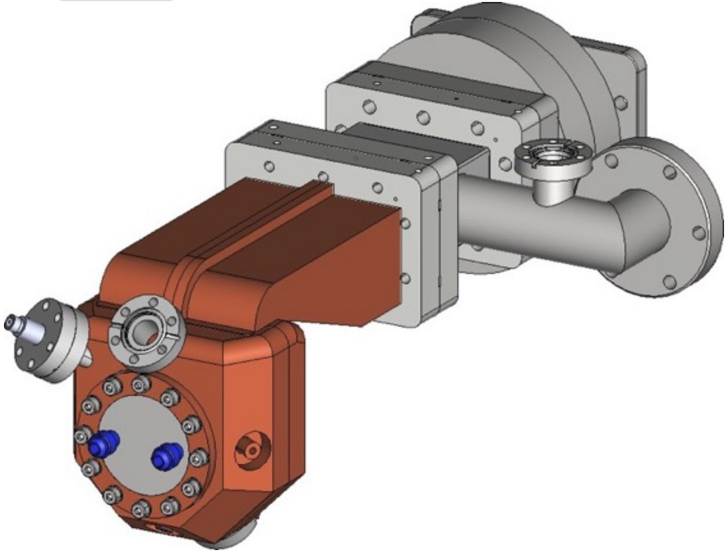

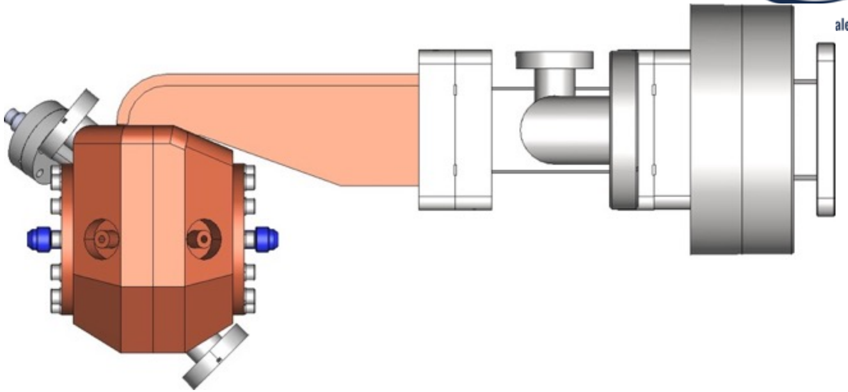

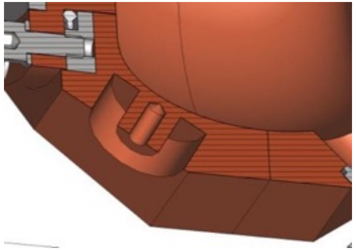

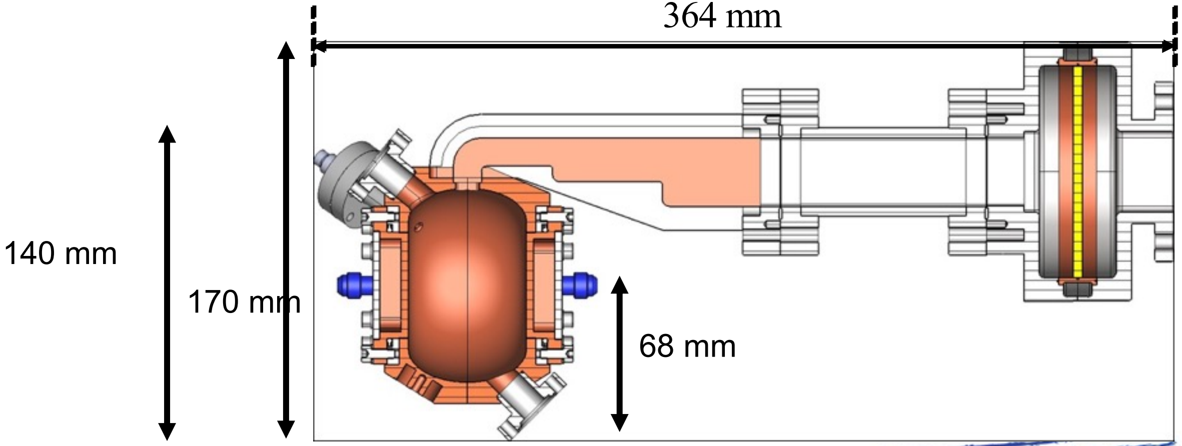

Windows for RF cavities

The 3 cells normal conducting cavity, shown in the last slides, consists of basic pillbox cavities which are enclosed with thin windows (foils) to increase shunt impedance and give a higher field on-axis for a given amount of power.

These windows are subject to ohmic heating from RF currents and Lorentz force from the EM field in the cavity, both of which will produce out of the plane displacements that can detune the cavity frequency.

Preliminary studies consider Berillium as a suitable material for these windows. Thickness ranging around tens of microns were considered for this application.

"THERMAL AND LORENTZ FORCE ANALYSIS OF BERYLLIUM WINDOWS FOR A RECTILINEAR MUON COOLING CHANNEL" T. Luo et al. IPAC 2015
"FINITE ELEMENT ANALYSIS OF THIN BERYLLIUM WINDOWS FOR A MUON COOLING CHANNEL"J. N. Corlett, N. Hartman, D. Li PAC 2001

Windows for RF cavities

The Be window needs to be thin enought to be almost transparent to the muon beam. However, the thinner the window, the poorer its thermal conduction. Besides, there is no extra cooling on the window with all the heat transfered out by thermal conduction.

Beryllium, moreover, requires a lot of attention in its handling and this makes very difficult both to find companies able in the production of these foils and, at the same time, prevent many laboratories to install small tes stand to study its properties.

Due to this reasons we are considering the possibility to use aluminium as an alternative material for these foils.

Windows for RF cavities

Index of Tables for Selected Chemical Elements

Element	Symbol	Z	A	State	ρ [g/cm^3]	$\langle -dE/dx \rangle_{\text{min}}$ [MeV cm^2/g]	$E_{\mu c}$ [GeV]	$\langle -dE/dx \rangle$ and range
Hydrogen gas	H	1	1.00794	D	8.375×10^{-5}	4.103	3611.	I–1
Liquid hydrogen	H	1	1.00794	L	7.080×10^{-2}	4.034	3102.	I–2
Helium gas	He	2	4.002602	G	1.663×10^{-4}	1.937	2351.	I–3
Liquid helium	He	2	4.002602	L	0.125	1.936	2020.	I–4
Lithium	Li	3	6.941	S	0.534	1.639	1578.	I–5
Beryllium	Be	4	9.012182	S	1.848	1.595	1328.	I–6
Boron	B	5	10.811	S	2.370	1.623	1169.	I–7
Carbon (compact)	C	6	12.0107	S	2.265	1.745	1056.	I–8
Carbon (graphite)	C	6	12.0107	S	1.700	1.753	1065.	I–9
Nitrogen gas	N	7	14.00674	D	1.165×10^{-3}	1.825	1153.	I–10
Liquid nitrogen	N	7	14.00674	L	0.807	1.813	982.	I–11
Oxygen gas	O	8	15.9994	D	1.332×10^{-3}	1.801	1050.	I–12
Liquid oxygen	O	8	15.9994	L	1.141	1.788	890.	I–13
Fluorine gas	F	9	18.9984032	D	1.580×10^{-3}	1.676	959.	I–14
Liquid fluorine	F	9	18.9984032	L	1.507	1.634	810.	I–15
Neon gas	Ne	10	20.1797	G	8.385×10^{-4}	1.724	906.	I–16
Liquid neon	Ne	10	20.1797	L	1.204	1.695	759.	I–17
Sodium	Na	11	22.989770	S	0.971	1.639	711.	I–18
Magnesium	Mg	12	24.3050	S	1.740	1.674	658.	I–19
Aluminum	Al	13	26.981538	S	2.699	1.615	612.	I–20

Windows for RF cavities

TABLE I-6. Muons in Beryllium

See page 209 for Explanation of Tables

Z	A [g/mol]	ρ [g/cm^3]	I [eV]	a	$k = m_s$	x_0	x_1	$\overline{C}$	δ_0
4 (Be)	9.012182	1.848	63.7	0.80392	2.4339	0.0592	1.6922	2.7847	0.14

T	p [MeV/c]	Ionization [MeV cm^2/g]	Brems [MeV cm^2/g]	Pair prod [MeV cm^2/g]	Photonucl [MeV cm^2/g]	Total [MeV cm^2/g]	CSDA range [g/cm^2]
10.0 MeV	4.704×10^{1}	6.491				6.491	8.616×10^{-1}
14.0 MeV	5.616×10^{1}	5.058				5.058	1.567×10^{0}
20.0 MeV	6.802×10^{1}	3.945				3.945	2.926×10^{0}
30.0 MeV	8.509×10^{1}	3.054				3.054	5.848×10^{0}
40.0 MeV	1.003×10^{2}	2.603				2.603	9.418×10^{0}
80.0 MeV	1.527×10^{2}	1.940				1.940	2.779×10^{1}
100. MeV	1.764×10^{2}	1.818				1.818	3.847×10^{1}
140. MeV	2.218×10^{2}	1.694				1.694	6.137×10^{1}
200. MeV	2.868×10^{2}	1.622				1.622	9.770×10^{1}
300. MeV	3.917×10^{2}	1.595			0.000	1.595	1.601×10^{2}

TABLE I-20. Muons in Aluminum

See page 209 for Explanation of Tables

Z	A [g/mol]	ρ [g/cm^3]	I [eV]	a	$k = m_s$	x_0	x_1	$\overline{C}$	δ_0
13 (Al)	26.981538	2.699	166.0	0.08024	3.6345	0.1708	3.0127	4.2395	0.12

T	p [MeV/c]	Ionization [MeV cm^2/g]	Brems [MeV cm^2/g]	Pair prod [MeV cm^2/g]	Photonucl [MeV cm^2/g]	Total [MeV cm^2/g]	CSDA range [g/cm^2]
10.0 MeV	4.704×10^{1}	6.188				6.188	9.151×10^{-1}
14.0 MeV	5.616×10^{1}	4.849				4.849	1.653×10^{0}
20.0 MeV	6.802×10^{1}	3.802				3.802	3.066×10^{0}
30.0 MeV	8.509×10^{1}	2.960				2.961	6.088×10^{0}
40.0 MeV	1.003×10^{2}	2.533				2.533	9.763×10^{0}
80.0 MeV	1.527×10^{2}	1.908				1.908	2.853×10^{1}
100. MeV	1.764×10^{2}	1.797				1.798	3.935×10^{1}
140. MeV	2.218×10^{2}	1.688				1.688	6.242×10^{1}
200. MeV	2.868×10^{2}	1.629				1.630	9.873×10^{1}
277. MeV	3.683×10^{2}	1.615			0.000	1.615	*Minimum ionization*
300. MeV	3.917×10^{2}	1.616			0.000	1.616	1.605×10^{2}

Windows for RF cavities

The pictures below show the result of a thermal analysis carried out on 4 different aluminum samples of thickness respectively of 50, 100, 200 and 300 microns.
The temperature raise ranges from 20 °C to 4°C.

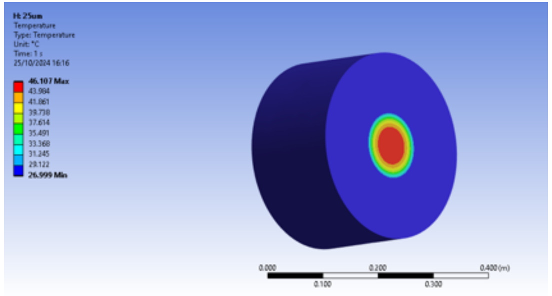

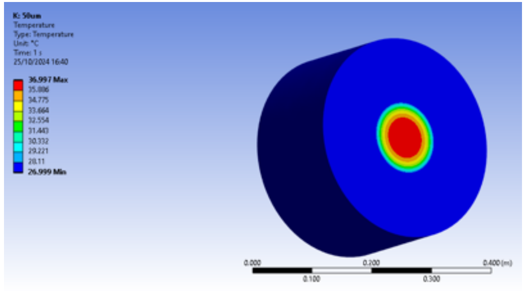

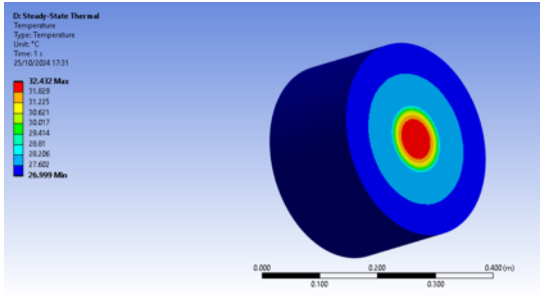

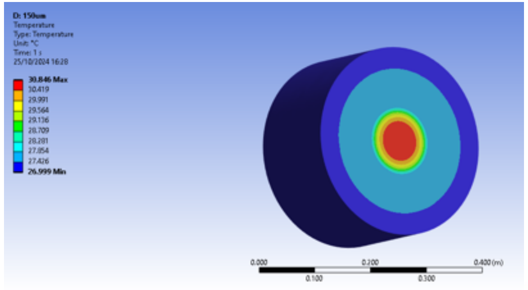

No significant increase from 200 to 300 micron

Windows for RF cavities

A “step” window design has been conceived as a compromise between emittance dilution and the thermal heating.

Preliminary analysis are underway with a step design with an anulus of 20 mm radial extension with 300 microns of height against a 100 micron foil.

ESPP-INFN New proposal in September 2024

Breakdown rate studies of normal conducting structures operating at electric fields > 30 MV/m up to 100 MV/m embedded in magnetic fields up to 10 T (mostly with E and B fields parallel to each other) represents one of the most exciting and relevant areas in the development of new proposals for accelerating machines.

The lack of experimental data and, as a consequence, the difficulties to develop and verify theoretical models of the involved phenomena must be addressed in a short period and this requires a significant effort involving an approach that will start from material science up to accelerator related advanced technologies.

The present proposal represents a unique opportunity in the area due to the possibility to take advantage in a short period of already existing testing facilities at LNF for RF power studies and the knowledge process under development at LASA related to the design of suitable magnet structures and RF cavities.

ESPP-INFN New proposal in September 2024

Design, specify and build (internally or commissioning to a company) a SC magnet feeded by a cryocooler and with a useful bore of 120 mm **to be used in the LNF TEX** facility for testing C and X band structures about the breakdown rate obtainable. The magnet will provide up to 4 T of magnetic field over a length of 200 mm.

Design, specify and build (commissioning to a company) **a couple of prototypes of single cells and power couplers** running at 704 MHz and 1 GHz and aimed for the Muon Collider (MC) project. These components will be tested at **low power in the RF laboratory under development at LASA within the previous ESPP funding**.

Design, specify and build (commissioning to a company) **a prototype of a full 3 RF cells element running at 704 MHz as the basic building block of the MC demonstrator structure**. Carry out low power tests at LASA and high power RF tests in a laboratory to be identified.

Design and build **a RF power coupler (up to few MW) for a 704 MHz and 1 GHz 3 RF cells structure.**

ESPP-INFN New proposal in September 2024

Design, specify and develop **a structure able to integrate a 7 T HTS based SC magnet with a full 3 RF cells elements as a prototype of the first cooling cell of the MC demonstrator structure**.

Continue **the technological developments underway at LASA and at LNL for the best materials and surface manipulation techniques to increase the breakdown rates and start studies that using the experimental results will allow to develop suitable theoretical studies of these phenomena**.

International
MUON Collider
Collaboration

CERN

Thank you for your attention

3 cells RF preliminary structure

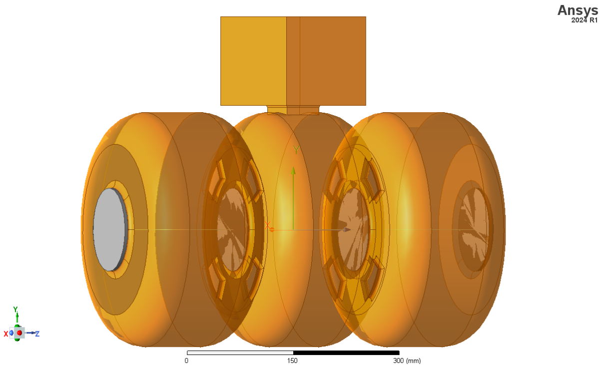

Figure 18: Design of 3 coupled cells centrally fed by a WR975 waveguide.

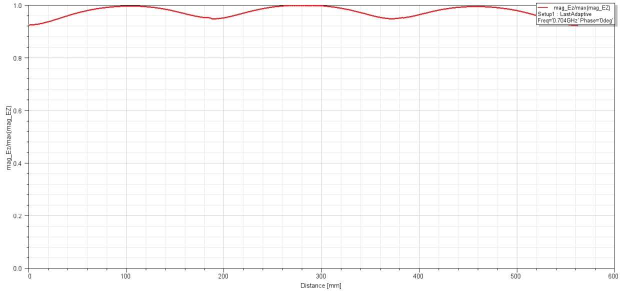

Figure 19: Electric field amplitude normalized to the max. $C_{R-1} = 46$, $C_{R0} = 50.25$ and $C_{R1} = C_{R-1}$ for the other geometric parameters refer to Tab. 6

The top circle curvature radius C_R is used to ensure the same accelerating gradient in the cells. In the plot C_R denotes the top circle curvature of the central cavity, whereas C_{R-1} and C_{R+1} denote the top circle curvature of the outer cavities.

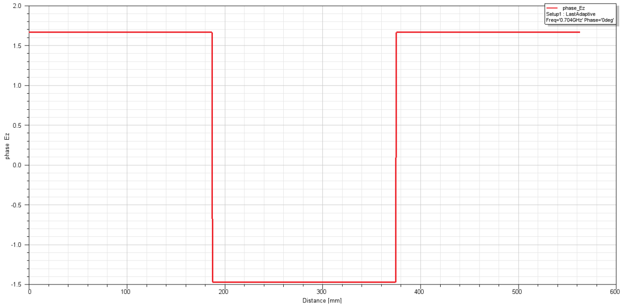

Figure 20: Electric field phase. $C_{R-1} = 46$, $C_{R0} = 50.25$ and $C_{R1} = C_{R-1}$

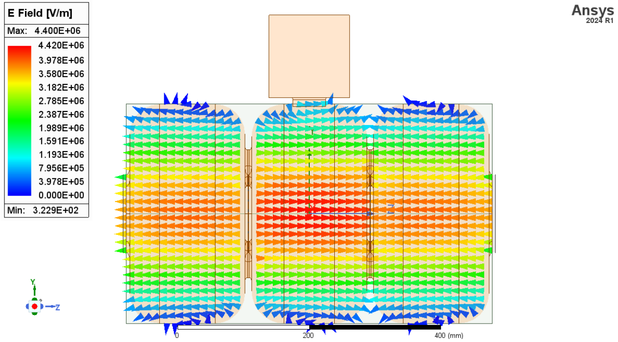

Figure 21: Electric Field Plot

References

[1] T. P. Wangler, *RF Linear accelerators*. John Wiley & Sons, 2008.